

Structural Heterogeneity in DNA: Temperature Dependence of 2-Aminopurine Fluorescence in Dinucleotides

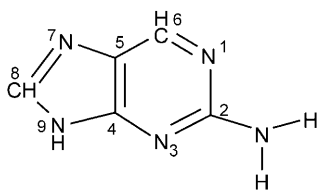
Oscar J. G. Somsen,* Linda B. Keukens, M. Niels de Keijzer, Arie van Hoek, and Herbert van Amerongen^[a]

The fluorescent base analogue 2-aminopurine is a sensitive probe for local dynamics of DNA. Its fluorescence is quenched by interaction with the neighboring bases, but the underlying mechanisms are still under investigation. We studied 2-aminopurine fluorescence in dinucleotides with each of the natural bases. Con-

sistently, two of the four fluorescence-decay components depend strongly on temperature. Our results indicate that these components are due to the excited-state dynamics of a single conformational state. We propose a variation of the gating model in which transient unstacking occurs in the excited state.

Introduction

2-Aminopurine (2AP) is a fluorescent base analogue. It can replace adenine in a DNA sequence without disrupting structure^[1–5] or function^[6–8] of the sequence. The structure of 2AP is shown in Scheme 1. 2AP is strongly fluorescent (quantum



Scheme 1. The structural formula of 2AP. This structure is similar to that of adenine. The only difference is that in the case of adenine the amino group is attached to the 6-carbon atom instead of to the 2-carbon atom.

yield: $\Phi = 66\%$ ^[9,10]) compared to the natural bases ($\Phi < 0.01\%$ ^[11,12]), but its fluorescence is strongly quenched in a DNA sequence. Thus, 2AP functions as a probe for interactions between neighboring bases. 2AP has been used to study mispair recognition,^[13–15] base flipping,^[16,17] local melting,^[1,6,7] protein binding,^[18–20] and electron transfer.^[21–24]

A four-exponential decay of 2AP fluorescence is often observed in DNA fragments.^[13,14,25] The fastest component (20–35 ps) has been attributed to a stacked conformation.^[14,15,26] The longest component (7–8 ns) may reflect a flipped conformation with 2AP twisted out of the helix.^[3,13,14,17] The intermediate components have been attributed to conformational transitions.^[22] But details of the conformations are unknown. Also the quenching mechanism itself is under discussion. O'Neill et al. only find fast decay in the presence of a neighboring guanine. They attribute this to electron transfer.^[22–24,27,28] In contrast, Rachofski et al. observe static (i.e. instantaneous) quenching by all natural bases.^[13] A dark state could also be involved.^[25,29,30,36]

We study how neighboring bases affect the fluorescence of 2AP. By using dinucleotides, we limit the interaction to a single neighboring base. The fluorescence decay is similar to that in larger DNA fragments.^[13,14,25] Herein, we analyze the temperature dependence of the fluorescence decay. As we will demonstrate, at least two decay components are due to excited-state dynamics. Our work provides information on local dynamics of DNA, and facilitates the use of 2AP as a probe.

Results

Figure 1 shows typical fluorescence curves fitted with a sum of exponential decay components. The fluorescence of monomeric 2AP can be fitted with a monoexponential decay of 7–10 ns. For the dinucleotides, at least four decay components are required. A fifth component improves the initial region of the fit. But this has little effect on the X^2 value. The residuals of a three-exponential fit are clearly nonrandom.

The fit results are shown in Table 1. Remarkably, the four decay components occur in distinct regions (18–35 ps, 0.3–0.8 ns, 1.8–3.1 ns and 8–9 ns). We shall call them components 1 to 4. Component 1 (18–35 ps) reflects fast quenching. Component 4 resembles monomeric 2AP, which could be due to degradation. However, its amplitude is larger than the specified sample impurity. Moreover, it does not vary between batches (not shown). Thus, component 4 reflects slow quenching in the dinucleotide.

Vibrational and solvent relaxation occurs on a sub-picosecond timescale in the dinucleotides.^[29] Thus, the observed components are not due to spectral shifts and can be interpreted

[a] Dr. O. J. G. Somsen, L. B. Keukens, M. N. de Keijzer, A. van Hoek, Prof. Dr. H. van Amerongen
Wageningen University, Laboratory of Biophysics
P.O. Box 8128, 6700 ET Wageningen (Netherlands)
Fax: (+31) 317-482725
E-mail: oscar.somsen@wur.nl

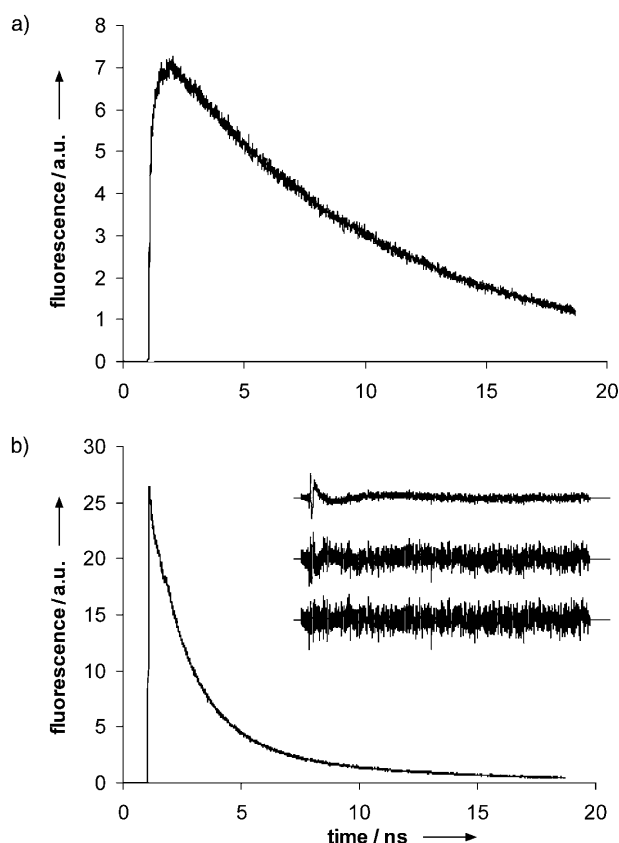


Figure 1. a) 2AP raw data (i.e. before deconvolution) with monoexponential fit. b) 2AP-guanine raw data with four-exponential fit. Inset: Residuals of a fit to 2AP-guanine with (Top to Bottom) three ($\chi^2=2.0$), four ($\chi^2=1.1$) and five ($\chi^2=1.0$) exponential decay components.

as decay of the excited state. This is supported by the fact that the position and shape of the steady-state fluorescence spectra is very similar for different dinucleotides,^[25] and does not change with temperature (not shown). Moreover, time-resolved fluorescence measurements on a 2AP-containing hairpin have shown that the fastest component is also due to excited-state decay.^[1]

Let us first consider the fluorescence of monomeric 2AP. From 20 to 60 °C the steady-state quantum yield decreases (0.66–0.49) as well as the fluorescence decay time (see Table 1). We can analyze this with a simple model that includes only quenching and fluorescence [see Eq. (2)]. The quenching rate increases with temperature [(19 ns)⁻¹–(14 ns)⁻¹]. The natural fluorescence rate does not change [(14.8 ns)⁻¹–(15.0 ns)⁻¹]. Thus, the strong temperature dependence of 2AP fluorescence is only due to a change in the quenching rate.

Next, we consider the fluorescence yields of the dinucleotides. Table 1 shows steady-state yields and estimates derived from the fit ($\Phi_{\text{fit}} = \sum_n p_n \tau_n / \tau_{2\text{AP}}$). As discussed earlier these should be equal if the fluorescence rate of 2AP has not changed in the dinucleotide.^[25] If components much faster than those in the table have been missed in the fit, the fit yield would be an overestimate. This is because the sum of the amplitudes is scaled to unity. In reality, the fit yields are somewhat smaller than the steady-state results, indicating that such fast components do not occur with significant amplitude.

Figure 2 illustrates the temperature dependence of the dinucleotide fit parameters. The temperature dependence of the amplitudes is characterised by a decrease of component 1 (the fastest decay component) and a corresponding increase of component 3. This is clearly seen in the figure. The amplitudes

of components 2 and 4 are largely constant within the experimental error. Some change is observed for the 2AP-guanine dinucleotide. The constancy of components 2 and 4 is not unexpected, at least if they are due to different states of the dinucleotide. This is because the range of (absolute) temperatures is not very large. The change of components 1 and 3, however, reflects strong temperature sensitivity.

The temperature dependence of the time constants is characterised by an approximately twofold speed-up of component 3. Component 1 shows an equally strong slow-down (except for 2AP-thymine). A minor change for component 4 resembles that of monomeric 2AP. This does not reflect changes in the dinucleotide. The speed-up of component 3 indi-

Table 1. Fit parameters for 2AP and five dinucleotides at three temperatures. Columns 3 to 6: Time constants (in ns) with the corresponding relative amplitude. Columns 7 and 8: Quantum yields (relative to monomeric 2AP) obtained from the fit parameters (see text) and the steady-state spectra (with excitation at 320 nm). Approximate uncertainties (obtained by comparison of two batches at room temperature): τ_1 (15%), τ_2 (10%), τ_3 (3%), τ_4 (2%), p_1 to p_4 (10%) and Φ_{rel} (10%).

Sample	Temp.	$\tau_1(p_1)$	$\tau_2(p_2)$	$\tau_3(p_3)$	$\tau_4(p_4)$	Φ_{fit}	Φ_{rel}
2AP	20 °C				9.8		
	40 °C				8.6		
	60 °C				7.3		
2AP-A	20 °C	0.031 (33)	0.59 (41)	2.1 (23)	8.3 (3.0)	0.099	0.124
	40 °C	0.042 (19)	0.54 (44)	1.5 (34)	7.4 (3.0)	0.115	0.123
	60 °C	0.050 (12)	0.50 (36)	1.2 (49)	6.4 (2.8)	0.132	0.147
2AP-C	20 °C	0.035 (48)	0.45 (14)	2.5 (36)	8.0 (2.0)	0.116	0.158
	40 °C	0.041 (34)	0.43 (15)	1.7 (49)	7.1 (1.9)	0.118	0.151
	60 °C	0.064 (25)	0.51 (14)	1.2 (59)	6.0 (1.9)	0.138	0.142
2AP-G	20 °C	0.025 (78)	0.33 (7)	1.8 (12)	8.8 (2.1)	0.045	0.065
	40 °C	0.018 (67)	0.31 (9)	1.2 (22)	7.6 (2.4)	0.056	0.053
	60 °C	0.030 (49)	0.48 (17)	0.9 (31)	6.3 (3.0)	0.067	0.056
2AP-I	20 °C	0.018 (35)	0.80 (20)	3.1 (39)	8.4 (5.9)	0.188	0.227
	40 °C	0.025 (21)	0.69 (22)	2.3 (52)	7.6 (5.0)	0.206	0.216
	60 °C	0.041 (5)	0.57 (19)	1.9 (71)	6.3 (5.7)	0.244	0.222
2AP-T	20 °C	0.025 (60)	0.38 (10)	2.4 (29)	8.2 (1.1)	0.086	0.098
	40 °C	0.025 (51)	0.35 (10)	1.6 (39)	7.6 (0.9)	0.085	0.092
	60 °C	0.026 (40)	0.29 (9)	1.1 (50)	6.3 (1.0)	0.099	0.094

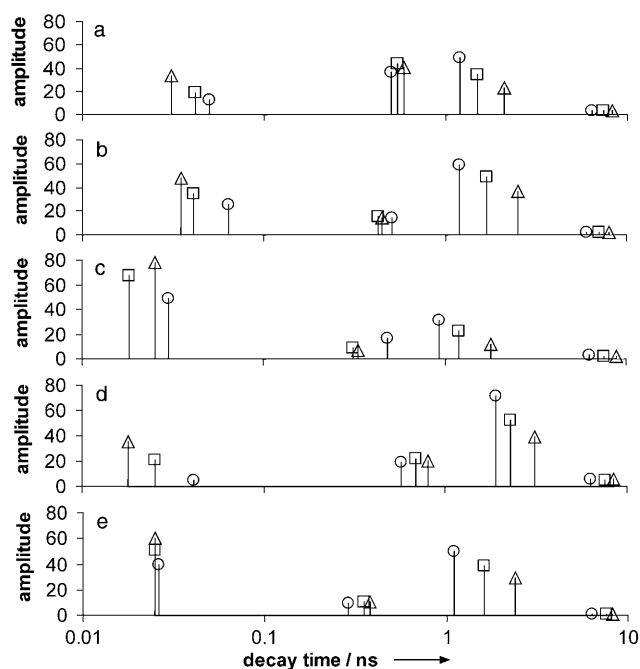


Figure 2. Graphical representation of Table 1. Shown are the amplitude and decay times of four exponential decay components at 20 °C (Δ), 40 °C (\square) and 60 °C (\circ). 2AP-X with X=adenine (a), cytosine (b), guanine (c), inosine (d) and thymine (e).

cates that this process has a relatively large activation energy [$\Delta E/k_B = 1690$ K, see Eq. (3)]. The slow-down of component 1 is remarkable. This could reflect increased heterogeneity of a stacked conformation.

The observed trends are similar for the dinucleotides. Components 1 and 3 depend strongly on temperature, while components 2 and 4 are relatively insensitive. Apparently, the four components have a different origin. We find the similarity between the dinucleotides surprising. It indicates that the underlying mechanisms are relatively independent of the bases involved. Below we shall attempt to clarify these mechanisms by searching for the simplest possible model for these common trends.

Discussion

The dinucleotides in our study show four-exponential decay of 2AP fluorescence. This was previously observed in larger DNA fragments.^[13,14] Surprisingly, component 4 was not observed in a study of trinucleotides.^[31] As discussed previously, the multi-exponential decay implies heterogeneity of the sample.^[25] We shall attempt to find a model for the temperature dependence of the decay components. In the simplest model each decay component corresponds to a state of the dinucleotide. The fitted amplitudes are proportional to the population of the corresponding state. By assuming thermal equilibrium, we can now calculate the free energy differences between the states [see Eq. (4) in the Experimental Section].

The results in Table 2 agree with a linear temperature dependence, that is, $\Delta G = \Delta E - T\Delta S$. From this, we can calculate

Table 2. Thermodynamic analysis of the four-state model. Shown are: $\Delta S/k_B$, $\Delta E/k_B$ and $\Delta G/k_B$ at three temperatures. All values are with respect to state 1. The uncertainty (derived from that of the fit parameters) is around 2 for ΔS and 600 K for ΔE .

Sample	State	$\Delta G/k_B$ [K] at 20 °C	$\Delta G/k_B$ [K] at 40 °C	$\Delta G/k_B$ [K] at 60 °C	$\Delta S/k_B$	$\Delta E/k_B$ [K]
2AP-A	2	-64	-263	-366	7.6	2150
	3	106	-182	-469	14	4312
	4	703	578	485	5.5	2299
2AP-C	2	361	256	193	4.2	1591
	3	85	-114	-286	9.3	2796
	4	931	903	858	1.8	1466
2AP-G	2	706	628	353	8.8	3298
	3	548	349	153	9.9	3449
	4	1059	1042	930	3.2	2004
2AP-I	2	164	-15	-445	15	4621
	3	-32	-284	-884	21	6208
	4	522	449	-44	14	4662
2AP-T	2	525	510	497	0.7	732
	3	213	84	-74	7.2	2318
	4	1172	1264	1228	-1.4	757

the energy and entropy differences. We find a strong cancellation of ΔE and ΔS . In terms of equilibrium, energy strongly favours one state and entropy the other. In the temperature range of our study the two exactly cancel for all four states. This appears to be too much of a coincidence. We conclude that the four-state model is not satisfactory. At least two of the four decay components should be due to excited-state dynamics.

Components 1 and 3 vary strongly with temperature, but the sum of their amplitudes does not change. Most likely, these two components correspond to a single ground state. We arrive at the three-state model in Figure 3. States 2 and 4

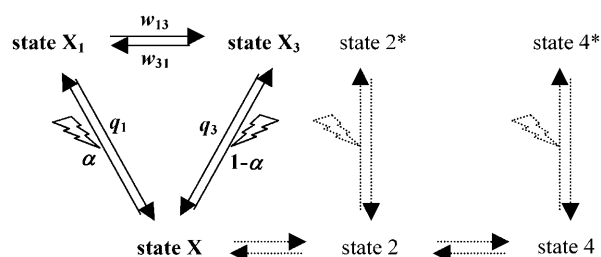


Figure 3. The three-state model. Here, α and $1-\alpha$ indicate the relative excitation of states X_1 and X_3 , q_1 and q_3 are the quenching rates in these states, and w_{13} and w_{31} are the transition rates between the two.

are each responsible for a single fluorescence decay component. State X has two relevant excited states, X_1 and X_3 . The total population of these two states shows a bi-exponential decay. This should be compared to components 1 and 3 of the data.

The analysis is simplified, because component 3 is much slower than component 1. The result is given in Equation (1), which is derived as shown in the Experimental Section:

$$\begin{aligned}
 k_1 &\approx q_1 + w_{13} \\
 p &\approx \alpha \frac{q_1}{q_1 + w_{13}} \\
 k_3 &\approx q_3 + \frac{q_1}{q_1 + w_{13}} w_{31}
 \end{aligned}
 \quad (1)$$

Here, $k_1 = 1/\tau_1$ and $k_3 = 1/\tau_3$ are the decay rates of components 1 and 3, respectively. And, $p = p_1/(p_1 + p_3)$ is the relative amplitude of component 1. The other parameters are defined in Figure 3.

Our model includes all transitions between X and its two excited states. Since Equation (1) has more than one solution we could select the most relevant transitions. First, note that both α , $q_1 \neq 0$. Else, $p \equiv 0$. Next, we may set $\alpha = 1$ or $w_{13} = 0$, but not both. Otherwise, $p \equiv 1$. In the former case, the temperature dependence of both k_1 and p can be reproduced by a change of q_1 . In the latter case, a change of at least two parameters is necessary. Therefore, the former provides the easiest explanation. Finally, either w_{31} or q_3 could individually be responsible for k_3 . The activation energy observed for k_3 (see Results section) is reproduced by w_{13} if X_3 is a relaxed state. This would imply that X_3 itself is hardly quenched.

We obtain a basic three-state model where X_1 is predominantly excited ($\alpha \approx 1$). Component 1 reflects fast quenching (q_1) and relaxation to X_3 (w_{13}). Component 3 could reflect reversal to X_1 (w_{31}). Our model is similar to the gating model that was proposed by O'Neill et al.^[22] and recently further substantiated.^[21,31] The main difference is that we propose that X_3 originates by relaxation from X_1 . O'Neill et al. assume that both states are present in the ground state. However, this cannot explain the temperature dependence in our study.

The above analysis is based on the temperature dependence of the fit parameters. One should note that fitting with four exponentials is a complex procedure. The obtained components could represent a distribution of decay times. However, the fact that the decay times obtained for the various dinucleotides occur in distinct regions, while the amplitudes are very different, indicates that the components represent distinct distributions. Also the largely consistent temperature dependence of the parameters, at least for components 1 and 3, indicates that relevant processes occur in those particular decay-time regions.

With the above approximations, Equation (1) has a unique solution. The results are shown in Table 3. While the model is an oversimplification, and the results should not be taken as quantitative, the transition rate w_{13} is surprisingly independent of temperature. This supports our suggestion that the decrease of k_1 and p with increasing temperature are both caused by a decrease of the quenching rate q_1 . As discussed above, w_{31} increases with increasing temperature.

Within the gating model X_1 to X_3 are distinct conformations. X_1 is a stacked well-quenched conformation. State X_3 is partially unstacked and needs restacking before it can be quenched.

Table 3. The rate parameters for the three-state model. As described in the text, the values were derived from the fit parameters in Table 1, with Equation (1) and simplifying assumptions $\alpha \equiv 1$ and $q_3 \equiv 0$.

Sample	Temp.	q_1 [ns ⁻¹]	w_{13} [ns ⁻¹]	w_{31} [ns ⁻¹]
2AP-A	20°C	19	13	0.8
	40°C	9	15	1.9
	60°C	4	16	4.2
2AP-C	20°C	16	12	0.7
	40°C	10	14	1.4
	60°C	5	11	2.8
2AP-G	20°C	35	5.3	0.6
	40°C	42	14	1.1
	60°C	20	13	1.8
2AP-I	20°C	26	29	0.7
	40°C	12	28	1.5
	60°C	2	23	8.0
2AP-T	20°C	27	13	0.6
	40°C	23	17	1.1
	60°C	17	21	2.0

On the basis of time-resolved absorption measurements on dinucleotides Larsen et al. also propose a 30–40 ps conformational transition from a well-quenched state to a state with a lifetime in the nanosecond range.^[29] Recent measurements on 2AP-containing trinucleotides have shown that the fluorescence decay components slow down with increasing viscosity.^[31] This also indicates that conformational transitions occur in the excited state.

What is distinctive here is the decrease of k_1 with increasing temperature. This is not due to viscosity, since that would cause an increase. Within the model described above it is due to a decrease of the fast quenching rate q_1 . This component could be due to electron transfer.^[27,28] However, comparison of time resolved absorption and fluorescence indicates that it could also involve formation of a dark state.^[25,29] In either case, its temperature dependence could be due to less-efficient stacking at high temperature.

In summary, we consistently find that two of the four fluorescence decay components depend strongly on temperature. Our results seem to rule out a model where each component is due to a separate state of the dinucleotide. The observed temperature dependence is most easily explained by assuming a highly quenched state that relaxes into a largely unquenched state. Quenching of this state requires reversal to the highly quenched state. The highly quenched state could be a stacked conformation of the dinucleotide. Our model indicates that this state partially unstacks after excitation.

Experimental Section

Dinucleotides (5' 2AP-X 3' with X = guanine, adenine, cytosine, thymidine or inosine) were purchased from Biolegio (Malden, Netherlands, purity > 99%). Monomeric 2AP was purchased from Sigma-Aldrich (purity > 99%). The samples were dissolved to OD₃₀₅

around 0.1 in 20 mM phosphate buffer (pH 7.0) with 100 mM NaCl. Steady-state spectra were recorded on Cary 5E (absorption) and Spex Fluorolog (fluorescence) spectrophotometers. All measurements were carried out in 10x4mm² fluorescence cuvettes (1.5 mL, Hellma).

Fluorescence decay curves were recorded with time-correlated single photon counting. Briefly, we used a laser (Coherent, Mira 900-D) with pulse picker, frequency tripler and Glan-laser polarizer to produce excitation pulses (0.2 ps, 290 nm, 3.8 MHz). Fluorescence was collected at 90° through a rotatable sheet polarizer and emission filter [374.6 nm, full width at half maximum (FWHM) = 7.8 nm] and detected by a microchannel plate photomultiplier (Hamamatsu R3809U-50). The arrival time of single photons was determined (with respect to a reference pulse) by a time-to-amplitude converter (Tennelec Inc., Oak Ridge, TS) and stored in a multichannel analyzer (4096 channels). The channel spacing was 6.98 ps.

To prevent pile-up, we reduced the count rate below 30 kHz using neutral-density filters in the excitation beam.^[32] Care was taken to minimize data distortion.^[33] The instrument response function (50 ps FWHM) was obtained from para-terphenyl in a 1:1 (volume) mixture of cyclohexane and CCl₄. A fresh sample was used for every recording. Temperature was regulated in the sample holder. Prolonged heating caused slow degradation of the sample. Thus, sample heating was limited to a few minutes, which was enough to obtain stable signals. Multiexponential fitting (including deconvolution of the instrument response) was done with home-written software.^[34,35]

Time-resolved fluorescence was, for technical reasons, recorded with excitation at 290 nm. While the neighboring bases are also excited at this wavelength, steady-state spectra indicate that fluorescence or transfer from these bases is very small.^[25] For steady-state fluorescence quantum yields the samples were excited at 320 nm.

To analyze the monoexponential fluorescence decay of monomeric 2AP, we used the standard model with parallel channels for quenching and (natural) fluorescence shown in Equation (2):

$$\Phi = k_f/k \quad \text{with} \quad k = k_f + k_q \quad (2)$$

Here, Φ and k are the observed fluorescence yield and decay rate, and k_f and k_q are the rates for natural fluorescence and quenching. When the former are known, the latter can be calculated. For description of an activated process we use Equation (3):

$$k \sim \exp(-\Delta E/k_B T) \quad (3)$$

where k is the rate, ΔE is the activation energy, k_B is the Boltzmann constant and T is the temperature. For description of an equilibrium between two states, we use Equation (4):

$$\frac{N_i}{N_j} \sim \exp\left(\frac{-\Delta G_{ij}}{k_B T}\right) \quad (4)$$

where N_i is the population of state i and ΔG_{ij} is the Gibbs free energy difference between states i and j .

Equation (1) is derived from the three-state model (see Figure 3). Components 1 and 3 of the observed fluorescence decay are due to total population of states X_1 and X_3 . The populations follow the rate Equation (5)

$$\frac{d}{dt} \begin{pmatrix} X_1 \\ X_3 \end{pmatrix} = M \begin{pmatrix} X_1 \\ X_3 \end{pmatrix} \quad \text{with} \quad M = \begin{pmatrix} -q_1 - w_{13} & w_{31} \\ w_{13} & -q_3 - w_{31} \end{pmatrix} \quad (5)$$

Here q_1 and q_3 are the quenching rates in the states X_1 and X_3 , respectively, and w_{13} and w_{31} are the transition rates between these two states (see also Figure 3).

The observed decay rates k_1 and k_3 correspond to the eigenvalues of the rate matrix M . The fractional amplitude p of the fast component is obtained by solving the rate equation with initial population ($\alpha, 1-\alpha$).

The results can be simplified because $k_3 \ll k_1$. First, consider the case where one eigenvalue is zero. All rate constants are non-negative and at least one of the quenching rates is nonzero. Thus, we obtain (without restricting generality): $q_3 = w_{31} = 0$. This simplifies the rate equation and leads to the expressions for k_1 and p in Equation (1). The expression for k_3 is obtained to first-order in q_3 and w_{31} .

Acknowledgements

Oscar Somsen and Herbert van Amerongen acknowledge financial support from the Foundation for Fundamental Research on Matter through Project no. 02ILP014.

Keywords: 2-aminopurine · DNA · fluorescence · structural heterogeneity · time-resolved spectroscopy

- [1] O. F. A. Larsen, I. H. M. van Stokkum, B. Gobets, R. van Grondelle, H. van Amerongen, *Bioph. J.* **2001**, *81*, 1115–1126.
- [2] S. M. Law, R. Eritja, M. F. Goodman, K. J. Breslauer, *Biochemistry* **1996**, *35*, 12329–12337.
- [3] T. M. Nordlund, S. Andersson, L. Nilsson, R. Rigler, A. Gräslund, L. W. McLaughlin, *Biochemistry* **1989**, *28*, 9095–9103.
- [4] L. C. Sowers, G. V. Fazakerley, R. Eritja, B. E. Kaplan, M. F. Goodman, *Proc. Natl. Acad. Sci.* **1986**, *83*, 5434–5438.
- [5] R. Eritja, B. E. Kaplan, D. Mhaskar, L. C. Sowers, J. Petruska, M. F. Goodman, *Nucleic Acids Res.* **1986**, *14*, 5869–5884.
- [6] A. Újvári, C. T. Martin, *Biochemistry* **1996**, *35*, 14574–14582.
- [7] K. D. Raney, L. C. Sowers, D. P. Millar, S. J. Benkovic, *Proc. Natl. Acad. Sci.* **1994**, *91*, 6644–6648.
- [8] L. W. McLaughlin, F. Benseler, E. Graeser, N. Piel, S. Scholtissek, *Biochemistry* **1987**, *26*, 7238–7245.
- [9] A. Holmén, B. Nordén, B. Albinsson, *J. Am. Chem. Soc.* **1997**, *119*, 3114–3121.
- [10] D. C. Ward, E. Reich, L. Stryer, *J. Biol. Chem.* **1969**, *244*, 1228–1237.
- [11] T. Gustavsson, A. Sharonov, D. Onidas, D. Markovitsi, *Chem. Phys. Lett.* **2002**, *356*, 49–54.
- [12] J. Peon, A. H. Zewail, *Chem. Phys. Lett.* **2001**, *348*, 255–262.
- [13] E. L. Rachofsky, E. Seibert, J. T. Stivers, R. Osman, J. B. A. Ross, *Biochemistry* **2001**, *40*, 957–967.
- [14] R. A. Hochstrasser, T. E. Carver, L. C. Sowers, D. P. Millar, *Biochemistry* **1994**, *33*, 11971–11979.
- [15] C. R. Guest, R. A. Hochstrasser, L. C. Sowers, D. P. Millar, *Biochemistry* **1991**, *30*, 3271–3279.
- [16] T.-J. Su, B. A. Connolly, C. Darlington, R. Mallin, D. T. F. Dryden, *Nucleic Acids Res.* **2004**, *32*, 2223–2230.
- [17] B. Holz, S. Klimasauskas, S. Serva, E. Weinhold, *Nucleic Acids Res.* **1998**, *26*, 1076–1083.
- [18] S. Roy, H. M. Lim, M. Liu, A. Sankar, *EMBO J.* **2004**, *23*, 869–875.
- [19] S. Shandrick, Q. Zhao, Q. Han, B. K. Ayida, M. Takahashi, G. C. Winters, D. V. Simonsen, T. Hermann, *Angew. Chem.* **2004**, *116*, 3239–3244; *Angew. Chem. Int. Ed.* **2004**, *43*, 3177–3182.
- [20] M. Kaul, C. M. Barbieri, D. S. Pilch, *J. Am. Chem. Soc.* **2004**, *126*, 3447–3453.
- [21] M. A. O'Neill, J. K. Barton, *J. Am. Chem. Soc.* **2004**, *126*, 11471–11483.

- [22] M. A. O'Neill, H.-C. Becker, C. Wan, J. K. Barton, A. H. Zewail, *Angew. Chem.* **2003**, *115*, 6076–6080; *Angew. Chem. Int. Ed.* **2003**, *42*, 5896–5900.
- [23] C. Wan, T. Fiebig, O. Schiemann, J. K. Barton, A. H. Zewail, *Proc. Natl. Acad. Sci.* **2000**, *97*, 14052–14055.
- [24] S. A. Kelley, J. K. Barton, *Science* **1999**, *283*, 375–381.
- [25] O. J. G. Somsen, A. van Hoek, H. van Amerongen, *Chem. Phys. Lett.* **2004**, *402*, 61–65.
- [26] K. B. Hall, D. J. Williams, *RNA* **2004**, *10*, 34–47.
- [27] M. A. O'Neill, C. Dohno, J. K. Barton, *J. Am. Chem. Soc.* **2004**, *126*, 1316–1317.
- [28] T. Fiebig, C. Wan, A. H. Zewail, *Chem. Phys. Chem.* **2002**, *3*, 781–788.
- [29] O. F. A. Larsen, I. H. M. van Stokkum, F. L. de Weerd, M. Vengris, C. T. Aravindakumar, R. van Grondelle, N. E. Geacintov, H. van Amerongen, *Phys. Chem. Chem. Phys.* **2004**, *6*, 154–160.
- [30] J. M. Jean, K. B. Hall, *Proc. Natl. Acad. Sci.* **2001**, *98*, 37–41.
- [31] J. M. Jean, K. B. Hall, *Biochemistry* **2004**, *43*, 10277–10284.
- [32] K. Vos, A. van Hoek, A. J. W. G. Visser, *Eur. J. Bioch.* **1987**, *165*, 55–63.
- [33] A. van Hoek, A. J. W. G. Visser, *Anal Instrum* **1985**, *14*, 359–378.
- [34] A. V. Digris, V. V. Skakun, E. G. Novikov, A. van Hoek, A. Claiborne, A. J. W. G. Visser, *Eur. Bioph. J.* **1999**, *28*, 526–531.
- [35] E. G. Novikov, A. van Hoek, A. J. W. G. Visser, J. W. Hofstraat, *Opt. Commun.* **1999**, *166*, 189–198.
- [36] O. F. A. Larsen, I. H. M. van Stokkum, M.-L. Groot, J. T. M. Kennis, R. van Grondelle, H. van Amerongen, *Chem. Phys. Lett.* **2003**, *371*, 157–163.

Received: December 21, 2004

Revised: April 21, 2005